Nigerian Research Journal of Chemical Sciences (ISSN: 2682-6054)
Volume 13, Issue 1, 2025

Synthesis and Characterization of $MgTiO_3$ Nanoparticles by Sol-Gel Method

*[1]Zalihat Abdullahi, [1]Jimoh Oladejo Tijani, [1]Alexander Ikechukwu Ajai,
[2]Ambali Saka Abdulkareem
[1]Department of Chemistry, Federal University of Technology, Minna, Niger State, Nigeria.
[2]Department of Chemical Engineering,
Federal University of Technology, Minna, Niger State, Nigeria.
*Corresponding Author: z.abdullahi@futminna.edu.ng

Accepted: April 26, 2025. Published Online: April 28, 2025

ABSTRACT

This study is on one-pot synthesis of magnesium titanate ($MgTiO_3$) nanoparticles via sol-gel route. The morphology, particles size, crystal structure, phase identification and functional groups of the produced nanomaterials were studied using high resolution scanning electron microscopy (HRSEM), X-ray diffraction (XRD) and Fourier transform infrared (FTIR) techniques. HRSEM analysis revealed characteristic homogeneous spherical shape for TiO_2 nanoparticles, while MgO and $MgTiO_3$ exhibited aggregated morphologies with irregular shapes with particle size 13.42 nm for TiO_2, 14.65 nm for MgO and 10.47 nm for $MgTiO_3$. XRD analysis established anatase phase of TiO_2, periclase phase for MgO, and mixture of the two phases for $MgTiO_3$ nanoparticles. Crystallite sizes calculated using Debye-Scherrer equation were 19.10 nm, 39.30 nm, and 17.51 nm for TiO_2, MgO and $MgTiO_3$ respectively. FTIR spectral profiles of TiO_2, MgO and $MgTiO_3$ show peaks for surface hydroxyl groups, molecular water, and metal-oxygen stretching. TiO_2 exhibits bands at 3300 cm^{-1} (O–H) and 670 cm^{-1} (Ti–O–Ti), MgO exhibited bands at 3400 cm^{-1} (O–H) and 603 cm^{-1} (Mg–O), while $MgTiO_3$ exhibited band at 3400 cm^{-1} (O-H) and at 614 cm^{-1} and 456 cm^{-1} (Ti–O–Mg–O). The resultant $MgTiO_3$ nanocomposite exhibited the desired characteristics, proving the sol-gel process to be a simple method for material preparation with promising applications in different fields.

Keywords: $MgTiO_3$, Sol-Gel, HRSEM, XRD, FTIR

INTRODUCTION

Nanotechnology has been area of extensive research for the past four decades owing to the application of materials unique physical, chemical, and biological properties in different fields [1, 2]. Nanoparticles are central to this area, and they are very tiny particles with sizes ranging from

1 to 100 nanometers [3]. These nanoparticles are fundamental building blocks of nanotechnology and have been found to possess wide-ranging applications in varied areas such as sensors, electronics, water treatment, cosmetics, biomedical implants, pharmaceuticals, environmental remediation, catalysis, and material science [4]. The unique characteristics of nanomaterials such as their smaller size, crystallinity, shape, high surface area-to-volume ratio, quantum confinement effects, and modified electronic structures greatly impact their catalytic, magnetic, electrical, and optical properties [5,6].

Titanium dioxide (TiO_2) nanoparticles have attracted much attention owing to its high chemical stability and multi-functional nature, making it an important ingredient in many commercial products. The anti-corrosive, photocatalytic, and optoelectronic characteristics of TiO_2 nanoparticle are accountable for its extensive application in plastics, paints, varnishes, paper, inks, personal care products, sunscreens, photovoltaic cells, wastewater treatment, and bactericidal applications [7]. The medical use of TiO_2 nanoparticle extends to photodynamic cancer treatment, drug delivery systems, cell imaging, biosensors for biological assays, and gene editing, demonstrating further its potential in contemporary technology.

Similarly, magnesium oxide (MgO) nanoparticles have attracted much attention due to their outstanding thermal stability, surface reactivity, heat resistance, and chemical inertness [8]. As an inorganic compound with a wide band gap of about 7.8 eV, MgO nanoparticle plays a significant role in catalysis and antimicrobial functions, particularly against foodborne pathogens. Due to their strong ionic nature, fixed stoichiometry, unique crystal structure, and defects in the surface structure, MgO nanoparticles displays great adsorption properties and therefore, are highly effective in wastewater treatment and poisonous gas removal from the environment [9]. Furthermore, they are biocompatible and non-toxic and hence are fit for biomedical applications and environmental cleanup.

Current developments in nanotechnology have led to the synthesis of various ceramic nanomaterials called titanates such as $PbTiO_3$, $SrTiO_3$, $BaTiO_3$, $FeTiO_3$, $CaTiO_3$, and $MgTiO_3$ which are used in a wide range of technical applications such as dielectric, pyroelectric, ferroelectric, piezoelectric, and optoelectronic.

Titanates are compound containing the titanate ion, TiO_3^{2-} which has excellent photocatalytic properties such as chemical stability, thermal stability, high charge separation and increased efficiency of pollutant degradation. Magnesium titanate ($MgTiO_3$) is a member of

perovskite nanostructures where Ti^{4+} ions are substituted with Mg^{2+}, introducing oxygen vacancies for charge neutrality. They are known to have unique properties such as increase surface area and quantum size effects as well as thermal and chemical stability, modified electronic and layered structure that facilitates greater charge separation [10, 11]. These properties make them effective for application in electronics, optics, photocatalysis, catalysis and in recent time in wastewater treatment.

Synthesis of nanomaterials employs diverse techniques, including chemical precipitation, thermal plasma, chemical vapour deposition, hydrothermal treatment, laser ablation, spray pyrolysis, ball-milling, sol-gel processes, and vacuum arc deposition. Of these, the sol-gel technique stands out with its low cost, ease of operation, and good control of nanoparticle size and shape [12]. Sol-gel approach entail steps such as hydrolysis, polymerization, evaporation, and condensation of metal salt precursors, leading to the creation of stable colloidal suspensions. One pot synthesis combines all reactant in a single reaction vessel to produce desired compound, reducing processing step and energy consumption.

In light of the importance of such nanomaterials, the current work seeks to synthesize TiO_2, MgO, and $MgTiO_3$ nanoparticles using one-pot sol-gel method and characterize the prepared nanomaterials using various analytical techniques

MATERIALS AND METHODS

Materials

Titanium (IV) isopropoxide ($Ti\{OCH(CH_3)_2\}_4$, 97%), magnesium nitrate hexahydrate ($Mg(NO_3)_2.6H_2O$, 99%) were purchased from Sigma Aldrich, Germany, sodium hydroxide (NaOH, 96%) and polyethylene glycol (PEG) were purchased from Lobie Chem. India. All chemicals used were of analytical grade, and all reagents were prepared in doubly distilled water.

Synthesis of TiO_2 Nanoparticles

TiO_2 nanoparticle was synthesized via sol gel method using $Ti\{OCH(CH_3)_2\}_4$ as precursor. In a typical synthesis, 16 cm^3 of $Ti\{OCH(CH_3)_2\}_4$ was added to 100 cm^3 of distilled water in a 250 cm^3 beaker. Exactly 10 cm^3 of 10 % (w/v) polyethylene glycol (PEG) was added and 0.5 mol/dm^3 NaOH was added dropwise to attain pH of 12. The mixture was stirred at 250 rpm for 1 h with heating at 60 °C until a gel was formed which was left overnight for ageing. After the ageing process, it was washed to a pH of 7 with distilled water and then oven dried for 8 h at 70

^oC. The powdered sample was calcined in a muffle furnace at a temperature of 450 ^oC for 3 h to obtain TiO_2 nanoparticles [13]

Synthesis of MgO Nanoparticles

MgO nanoparticle was synthesized via sol gel method using $Mg(NO_3)_2.6H_2O$ as precursor. In a typical synthesis, 7.7 g of $Mg(NO_3)_2.6H_2O$ was added to 100 cm^3 of distilled water. Exactly 10 cm^3 of 10 % (w/v) polyethylene glycol was added and 0.5 mol/dm^3 NaOH was added dropwise to attain pH of 12. The mixture was stirred at 250 rpm for 1 h with heating at 60 °C until a gel was formed which was left overnight for ageing. After the ageing process, it was washed to a pH of 7 with distilled water and then oven dried for 8 h at 70 ^oC. The obtained powdered sample was calcined in a muffle furnace at a temperature of 450 ^oC for 3 h to obtain MgO nanoparticles [13].

One-Pot Synthesis of $MgTiO_3$ Nanoparticles

The one pot synthesis of $MgTiO_3$ nanoparticle was carried out using $Mg(NO_3)_2.6H_2O$ and $Ti\{OCH(CH_3)_2\}_4$, as precursors via sol-gel process. In a typical procedure, 7.7 g of $Mg(NO_3)_2.6H_2O$ was weighed and added to 100 cm^3 of distilled water in a 250 cm^3 beaker followed by adding 16 cm^3 of $Ti\{OCH(CH_3)_2\}_4$. 10 cm^3 of 10 % (w/v) polyethylene glycol (PEG) was added as a stabilizing agent and 0.5 mol/dm^3 NaOH was added dropwise to adjust the pH to 12. The mixture was stirred at 250 rpm for 1 h with heating at 60 °C until a gel was formed which was left overnight for ageing. After the ageing process, it was washed to a pH of 7 with distilled water and then oven dried for 8 h at 70 ^oC. The obtained powder sample was calcined in a muffle furnace at a temperature of 450 ^oC for 3 h to obtain $MgTiO_3$ nanoparticles [13]

Characterization of the Synthesized Nanomaterials

The structure and morphology of the synthesized nanomaterials were examined with Zeiss Auriga high-resolution scanning electron microscopy (HRSEM). The crystal phase was studied with powder X-ray diffraction (XRD) Bruker AXS D8 Advance X-ray Diffractometer (Cu Kα radiation, wavelength 1.5418 Å), and the functional groups of the synthesized material were analyzed using Fourier transform infrared (FTIR) spectroscopy, and the spectra were recorded on a Shimadzu FTIR-spectrophotometer at the range of 400-5000 cm^{-1}.

RESULTS AND DISCUSSION

HRSEM

HRSEM micrograph of TiO_2 nanoparticle in Figure 1(a) shows a spherical particle with little agglomeration indicating that the nucleation and growth methodology of TiO_2 nanoparticles controlled the formation of the grain size and morphology [14]. The average particle size is found to be 13.42 nm.

Figure 1(b) shows the HRSEM micrograph of MgO nanoparticles. They are irregular spherical particles with slight agglomeration having average particle size of 14.65 nm. Salman et al [15] reported the synthesis of MgO nanoparticle prepared by the microwave and sol-gel approaches to have average grain size of approximately 50 nm and 72 nm indicating that, synthesis methods applied to MgO nanoparticles greatly determine their shape and size. Similarly, Abinaya and Kavitha, [16], pointed the effect of different method of synthesis on the morphology of MgO nanoparticle which is due to the surface energy and size.

The HRSEM micrograph of $MgTiO_3$ nanoparticles shown in Figure 1(c), indicates a uniformly distributed spherical particles with little agglomeration with a particle size of 10.47 nm. This agglomeration may be due to strong interparticle interactions such as van der Waals forces and electrostatic attractions and also variations in ionic radii and diffusion rates of the constituent elements [17].

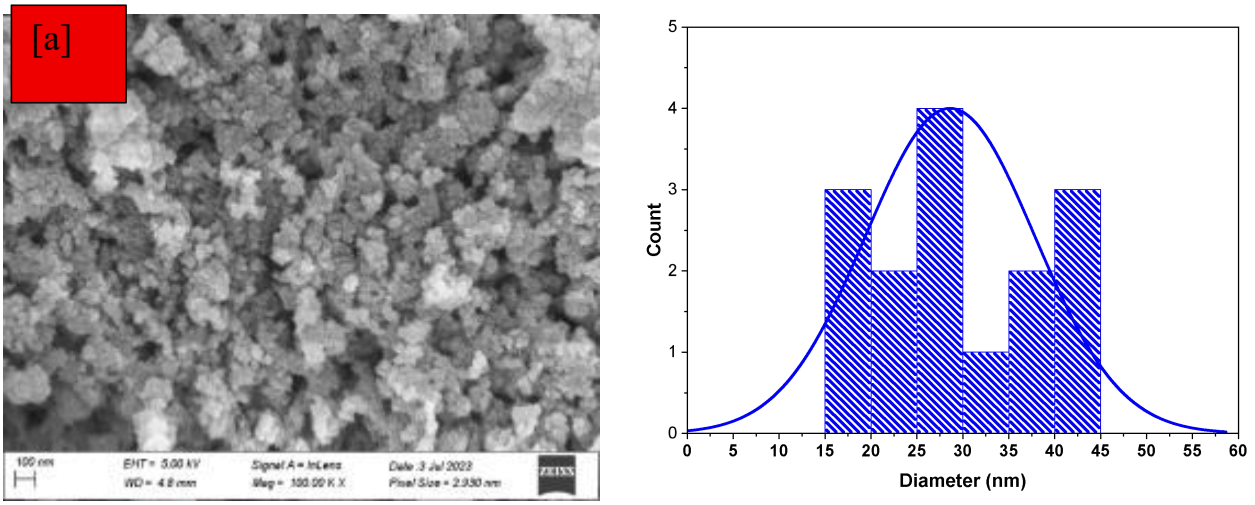

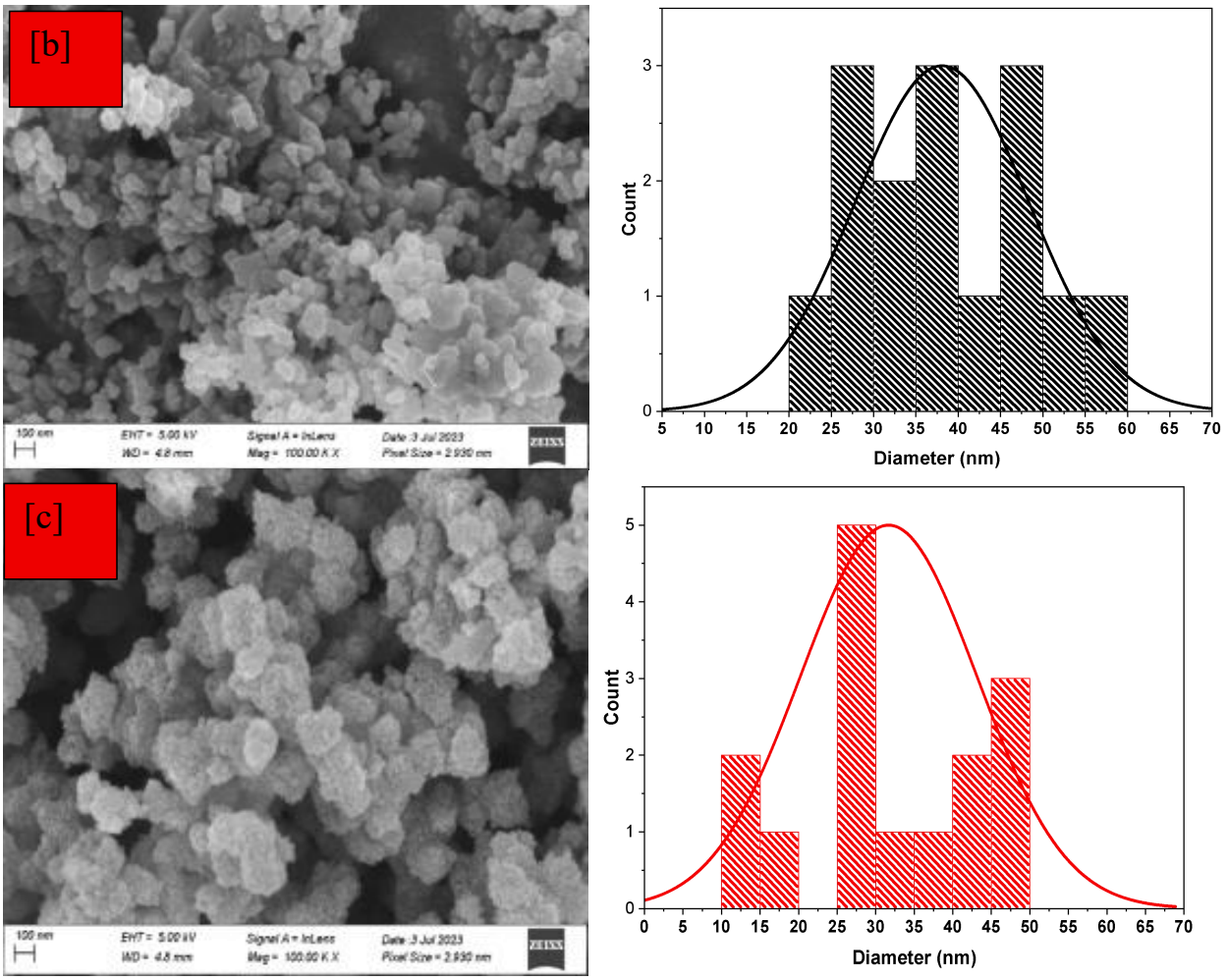

Figure 1: HRSEM Micrograph (a) TiO_2 (b) MgO (c) $MgTiO_3$ Nanoparticles

XRD

Figure 2 shows the XRD spectra of TiO_2, MgO, and $MgTiO_3$ nanoparticles reflecting their distinct crystalline phases.

The diffraction pattern of TiO_2 nanoparticles has distinct peaks of the anatase phase, with 2θ values of 25.45°, 37.77°, 47.57°, 54.79° and 62.44° which are attributed to the crystal planes of (101), (004), (200), (211) and (204), according to the Joint Committee on Powder Diffraction Standards (JCPDS) card number 21-1272.

MgO nanoparticles diffraction pattern contain characteristic peaks appearing at 2θ positions of 6.9°, 42.9°, 62.3°, 74.7°, and 78.6° corresponding to 111, 200, 220, 311, and 222 planes, respectively which are in accordance with JCPDS card number 65-0476, and this indicates the presence of periclase MgO nanoparticle, while the XRD pattern of $MgTiO_3$ shows

peaks at 2θ values of 27°, 38°, 41°, 54°, and 56° for the 214, 309, 232, 223, and 321 crystal planes, respectively which correspond to the JCPDS card number 02-0874 indicating the presence of mixture of two phases for $MgTiO_3$. The residual peaks observe in the XRD pattern of $MgTiO_3$ may be due to the presence of MgO and TiO_2 phases in the sample pointing towards the presence of both phases in the sample. The crystallite sizes were calculated using the Debye-Scherrer equation (Equation 1) to be 19.10 nm, 39.30 nm and 17.51 nm for TiO_2, MgO and $MgTiO_3$. Comparing the observed crystallite sizes to other works, Mustapha et al [18] synthesized TiO_2 nanoparticles by the sol–gel process from titanium (IV) isopropoxide and sodium hydroxide and the crystallite size was estimated to be 12.34 nm, indicating that strain effects contribute little to broadening the diffraction peaks consistent with the anatase phase of TiO_2. Similarly, Sim et al [19] used the sol gel method for the synthesis of MgO nanoparticle and the crystallite size was found to be 18.92 nm. In the present work, it is evident that crystallite size in $MgTiO_3$ decreased when compared to that of TiO_2 and MgO. This may be due to lattice strain and defects and also due to Mg-Ti ion interaction which may affect nucleation and growth kinetics, resulting in smaller crystallite sizes. Furthermore, the structural complexity of $MgTiO_3$ over TiO_2 and MgO could also lead to retarded grain development and increased structural disorder, further restricting crystallite size.

$$D = \frac{k\lambda}{\beta\cos\theta} \qquad (1)$$

where D is the crystallite size (nm), k is a constant (0.94), λ is the wavelength of the X-ray radiation (CuKaα = 0.1541 nm), β is the full width at half maximum (FWHM) of the intense and broad peaks and θ is the Bragg's or diffraction angle.

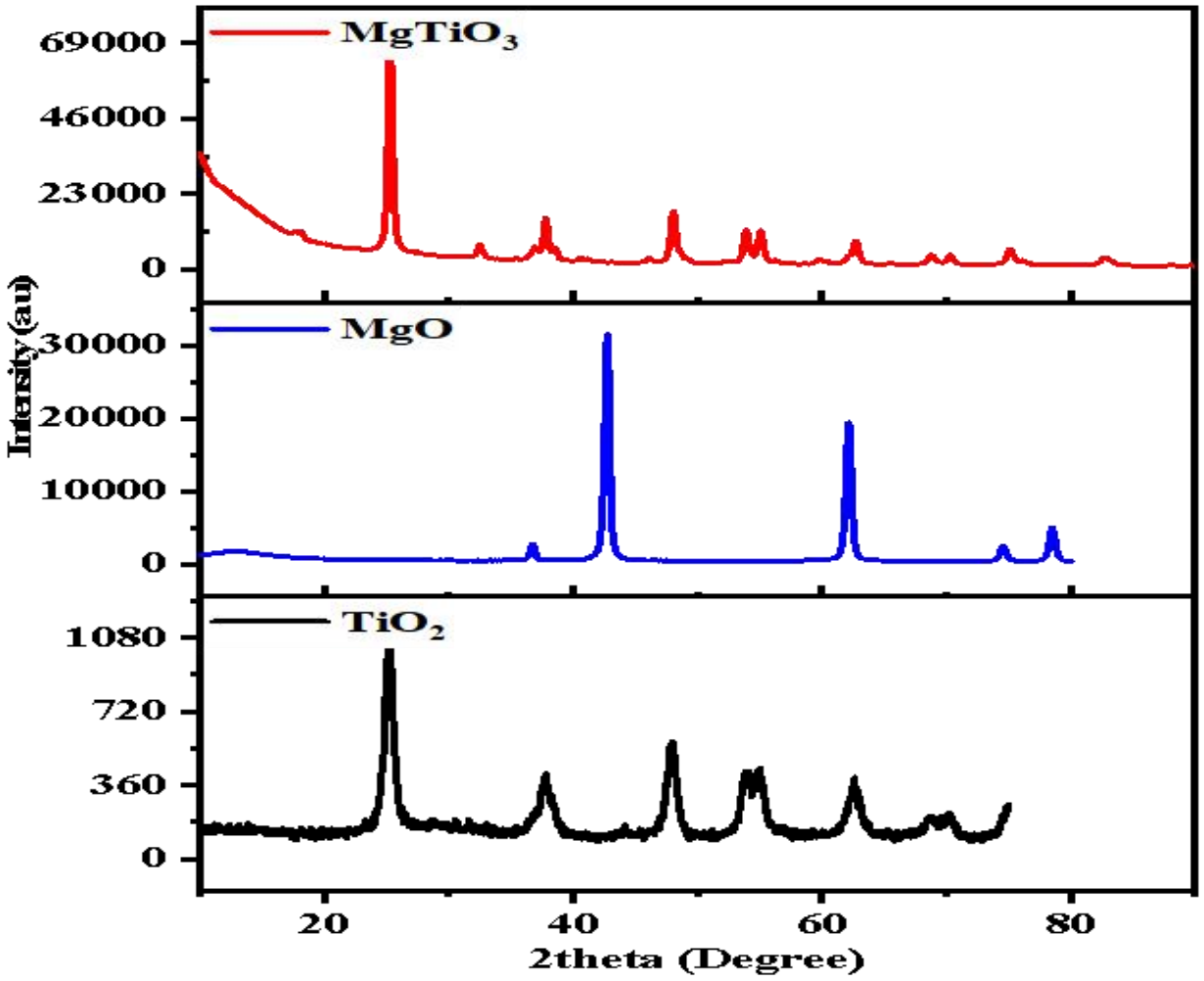

Figure 2: XRD Pattern of (a) TiO_2 (b) MgO (c) $MgTiO_3$

FTIR

The FTIR spectra of MgO, TiO_2, and $MgTiO_3$ nanoparticles are shown in Figure 3. TiO_2 shows characteristic absorption bands at 3400 cm^{-1}, 1630 cm^{-1}, 603 cm^{-1}, and 489 cm^{-1}. The broad band at 3400 cm^{-1} is attributed to the O–H stretching vibration of surface hydroxyl groups due to adsorbed water molecule. Ghoniem et al [20], also reported an intense band at 3438 cm^{-1} attributed to the TiO_2 nanorods O–H group stretching vibration, which is in good agreement with the 3400 cm^{-1} band reported in this work. In addition, [21] noticed a wide absorption band in the range of 3300–3600 cm^{-1}, showing the presence of hydroxyl groups generated during TiO_2 synthesis. This suggests that the presence of hydroxyl groups and water adsorbed is a feature of TiO_2 nanomaterials as also reported in previous studies [22, 23]

The bending vibration of H causes the band at 1630 cm^{-1}–O–H of molecular water. The peaks at 603 cm^{-1} and 489 cm^{-1} are attributed to the Ti–O stretching vibrations, which are characteristic of TiO_2 lattice vibrations. MgO reveals absorption bands at 3300 cm^{-1}, 1650 cm^{-1}, 1430 cm^{-1}, 670 cm^{-1}, and 580 cm^{-1}. The bands at 3300 cm^{-1} and 1650 cm^{-1} are attributed to O–H stretching and bending vibrations of adsorbed water, respectively. The band at 670 cm^{-1} and 580 cm^{-1} correspond to Mg–O stretching vibrations, typical of the Mg–O crystal lattice. $MgTiO_3$ shows absorption bands at 3400 cm^{-1}, 1456 cm^{-1}, 1138 cm^{-1}, 614 cm^{-1}, and 456 cm^{-1}. The peak at 3400 cm^{-1} is due to O–H stretching of water adsorbed, and the band at 1456 cm^{-1} is attributable to C-H bending vibration. The bands at 614 cm^{-1} and 456 cm^{-1} are due to metal-oxygen stretching (Ti–O–Mg–O).

The presence of hydroxyl group on the surface of the synthesized nanomaterials maybe attributed to the high surface area and reactivity of nanoparticles resulting in surface hydroxylation

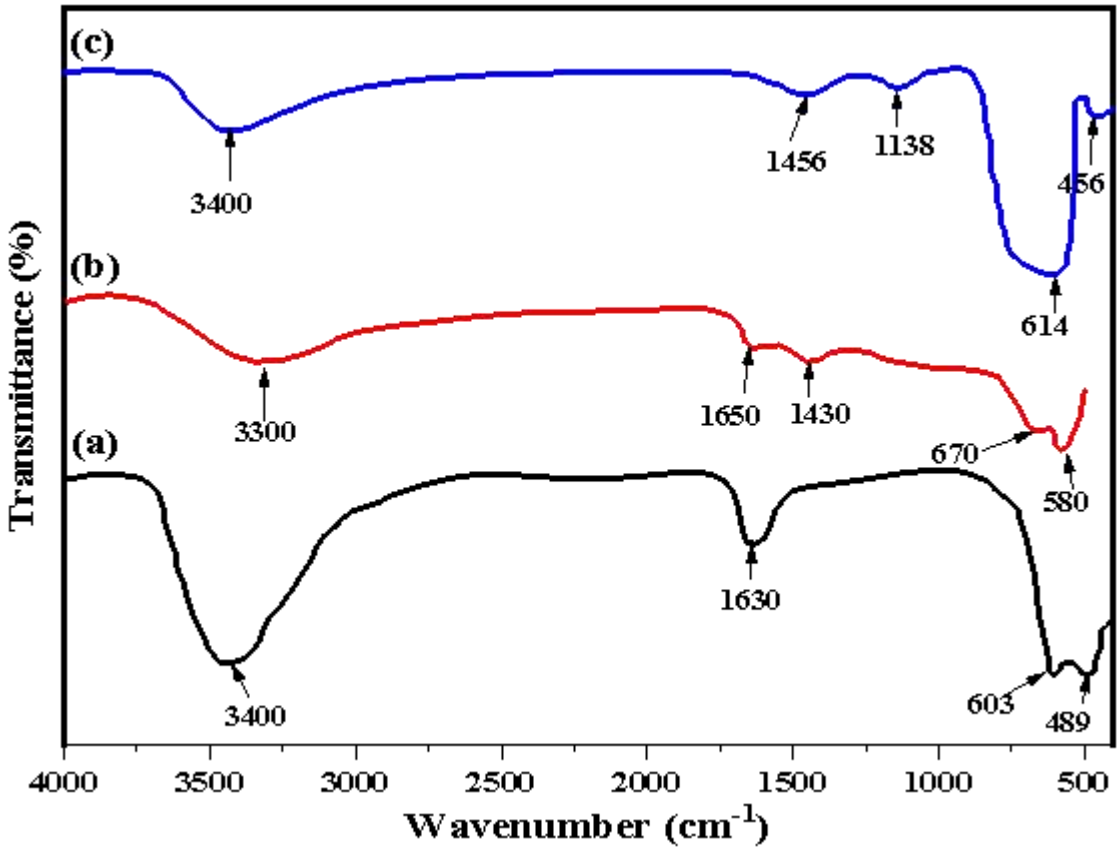

Figure 3: FTIR Spectra (a) TiO_2 (b) MgO (c) $MgTiO_3$ nanoparticles

CONCLUSION

The one-pot synthesis of $MgTiO_3$ particle was conducted via sol gel method and was compared with TiO_2 and MgO. The nanomaterials were characterized using HRSEM, XRD and FTIR. The HRSEM study revealed the morphological features of TiO_2, MgO, and $MgTiO_3$ nanoparticles, driven by synthesis conditions and processing parameters. TiO_2 is homogeneously nano-spherical in morphology, while MgO and $MgTiO_3$ showed irregular morphologies with little agglomeration. Particle shape and size variations are related to parameters such as calcination time, precursor concentration, and nucleation processes. XRD analysis confirmed the crystalline phases of TiO_2, MgO, and $MgTiO_3$ with diffraction patterns in agreement with JCPDS standards. Crystallite size calculations indicated lower crystallite size for $MgTiO_3$ compared to TiO_2 and MgO which may be due to structural complexity, lattice strain, defects, and ion-ion interactions that affect nucleation and growth kinetics. The existence of residual MgO and TiO_2 peaks in the $MgTiO_3$ XRD pattern, indicates incomplete phase transformation. FTIR measurement identified the characteristic functional groups in TiO_2, MgO and $MgTiO_3$. Hydroxyl groups and adsorbed water molecules were present in all the materials, represented by broad O–H stretching bands. Individual metal-oxygen vibrations were observed in TiO_2, MgO but $MgTiO_3$ has mixed metal-oxygen interactions. The findings emphasize the contribution of structural complexity on the crystallite size and grain evolution, offering insights into the phase composition and material characteristics of $MgTiO_3$ nanoparticle that can influence its applications across diverse areas.

REFERENCES

1 Himel, M. H., Sikder, B., Ahmed, T. & Choudhury, S. M. (2023). Biomimicry in Nanotechnology: A Comprehensive Review. *Nanoscale Advances*, *5*(3), 596-614.

2 Szczyglewska, P., Feliczak-Guzik, A. & Nowak, I. (2023). Nanotechnology–general Aspects: A Chemical Reduction Approach to the Synthesis of Nanoparticles. *Molecules*, *28*(13), 4932.

3 Modena, M. M., Rühle, B., Burg, T. P. & Wuttke, S. (2019). Nanoparticle Characterization: What to Measure. *Advanced Materials*, *31*(32), 1901556.

4 Taha, T. B., Barzinjy, A. A., Hussain, F. H. S. & Nurtayeva, T. (2022). Nanotechnology and Titanium Dioxide Nanoparticles under Different pH Conditions. *Journal of Engineering*, *25*(1), 40-50.

5 Khan, S. & Hossain, M. K. (2022). Classification and Properties of Nanoparticles. In *Nanoparticle-Based Polymer Composites*, 15-54.

6 Negrescu, A. M., Killian, M. S., Raghu, S. N., Schmuki, P., Mazare, A. & Cimpean, A. (2022). Metal Oxide Nanoparticles: Review of Synthesis, Characterization and Biological Effects. *Journal of Functional Biomaterials*, *13*(4), 274.

7 Nagaraj, K., Radha, S., Deepa, C. G., Raja, K., Umapathy, V., Badgujar, N. P., Parekh, N. M., Manimegalai, T., Devi, L. A. & Uthra, C. (2025). Photocatalytic Advancements and Applications of Titanium Dioxide (TiO_2): Progress in Biomedical, Environmental, and Energy Sustainability. *Next Research*, 100180.

8 Perera, H. C. S., Gurunanthanan, V., Singh, A., Mantilaka, M. M. M. G. P. G., Das, G. & Arya, S. (2024). Magnesium Oxide (MgO) Nanoadsorbents in Wastewater Treatment: A Comprehensive Review. *Journal of Magnesium and Alloys*.

9 Yadav, P., Saini, R. & Bhaduri, A. (2023). Facile Synthesis of MgO Nanoparticles for Effective Degradation of Organic dyes. *Environmental Science and Pollution Research*, *30*(28), 71439-71453.

10 Sneha, Y., Yashas, S. R., Thinley, T., Prabagar Jijoe, S. & Puttaiah Shivaraju, H. (2022). Photocatalytic Degradation of Lomefloxacin Antibiotics using Hydrothermally Synthesized Magnesium Titanate under Visible Light-driven Energy Sources. *Environmental Science and Pollution Research*, *29*(45), 67969-67980.

11 Wolde, G. S., Kuo, D. H. & Abdullah, H. (2022). Solar-light-driven Ternary $MgO/TiO_2/g\text{-}C_3N_4$ Heterojunction Photocatalyst with Surface Defects for Dinitrobenzene Pollutant Reduction. *Chemosphere*, *307*, 135939.

12 Saleh, H. M. & Hassan, A. I. (2023). Synthesis and Characterization of Nanomaterials for Application in Cost-effective Electrochemical Devices. *Sustainability*, *15*(14), 10891.

13 Shaba, E. Y., Tijani, J. O., Jacob, J. O. & Suleiman, M. A. T. (2022). Adsorptive Potential of ZnO/SiO_2 Nanorods Prepared via the Sol–Gel Method for the Removal of Pb (II) and Cd (II) from Petroleum Refinery Wastewater. *Journal of Chemical Technology & Biotechnology*, *97*(8), 2196-2217.

14 Abdulmajeed, B. A., Hamadullah, S. & Allawi, F. A. (2019). Synthesis and Characterization of Titanium Dioxide Nanoparticles under Different pH Conditions. *Journal of Engineering*, *25*(1), 40-50.

15. Salman, K. D., Abbas, H. H. & Aljawad, H. A. (2021). Synthesis and Characterization of MgO Nanoparticle via Microwave and Sol-gel Methods. In *Journal of Physics: Conference Series* 1973(1), 012104.

16 Abinaya, S. & Kavitha, H. P. (2023). Magnesium Oxide Nanoparticles: Effective Antilarvicidal and Antibacterial Agents. *ACS omega*, *8*(6), 5225.

17 Khairunnisa, S., Wonoputri, V. & Samadhi, T. W. (2021). Effective Deagglomeration in Biosynthesized Nanoparticles: A Mini Review. In *IOP Conference Series: Materials Science and Engineering* 1143(1), 012006.

18 Mustapha, S., Tijani, J. O., Ndamitso, M. M., Abdulkareem, A. S., Shuaib, D. T., Amigun, A. T. & Abubakar, H. L. (2021). Facile Synthesis and Characterization of TiO_2 Nanoparticles: X-ray Peak Profile Analysis using Williamson–Hall and Debye–scherrer Methods. *International Nano Letters*, *11*(3), 241-261.

19 Sim, H. T., Gençaslan, M. & Merdan, M. (2024). Synthesis of MgO nanoparticles via the Sol-gel Method for Antibacterial Applications, Investigation of Optical Properties and Comparison with Commercial MgO. *Discover Applied Sciences*, *6*(11), 1-11.

20 Ghoniem, M. G., Ali, F. A. M., Abdulkhair, B. Y., Elamin, M. R. A., Alqahtani, A. M., Rahali S. & Ben-Aissa, M. A. (2022). Highly Selective Removal of Cationic Dyes from Wastewater by MgO Nanorods. *Nanomaterials*, *12*(6), 1023.

21 Koshy, R. R., Reghunadhan, A., Mary, S. K., Pothen, L. A. & Thomas, S. (2022). MgONP/Chitin Nanowhisker-Based Hybrid Filler Bound Soy Protein Thin Films for Bioactive Packaging Applications. *International Journal of Food Science and Technology*, *57*(9), 5650-5662.

22 Sasi, S., Chandran, A., Sugunan, S. K., Krishna, A. C., Nair, P. R., Peter, A. & Mathew, S. (2022). Flexible Nano-TiO_2 Sheets Exhibiting Excellent Photocatalytic and Photovoltaic Properties by Controlled Silane Functionalization; Exploring the New Prospects of Wastewater Treatment and Flexible DSSCs. *ACS omega*, *7*(29), 25094-25109.

23. Zhao, Z., Jin, X., Liang, Y., Wang, L. M. & Liu, Y. D. (2022). TiO_2 Nanoparticles Dual-modified with Ionic Liquid and Acetic Acid for use as Electrorheological Materials to Achieve Ultrahigh and Stable Electroresponsive Performances. *ACS Applied Nano Materials*, *5*(12), 17928-17938.